Mechanism of carrier photogeneration in amorphous selenium: Fast transient photoconductivity

Daniel Moses
Institute for Polymers and Organic Solids, University of California, Santa Barbara, California 93106
(Received 13 February 1995)

Studies of fast transient photoconductivity in amorphous selenium reveal two distinct transport mechanisms. The first is a short-lived one due to carrier dynamics at extended band states and possibly states near the band edges where the carriers tunnel progressively into lower states. The second is a long-lived one due to phonon assisted multiple trapping at band tails. We find the quantum efficiency in this prototypic low-mobility system independent of temperature and electric field up to the maximum applied field of 5×10^5 V/cm, inconsistent with previous models of carrier photogeneration such as the Onsager geminate recombination model. In order to reconcile the controversial issue of the carrier photogeneration mechanism in this material, we examine in detail the processes underlying various transient photoconductivity measurements. Our analysis shows that in time-of-flight and xerographic-discharge measurements the external field may modify the extent of carrier recombination and thereby determines the carrier supply yield, whereas measurements utilizing the microstripline Auston switch configuration are better suited for investigating the intrinsic properties of the quantum efficiency.

I. INTRODUCTION

In the last decade, considerable effort has been devoted to unraveling the three generic aspects of transient photoconductivity in the class of low-mobility materials: carrier photogeneration, carrier mobility, and carrier recombination. Short laser pulses, matched microstripline configurations[1] (MSS), and fast electronic signal detection systems have opened the subnanosecond to picosecond time domain, thereby facilitated the advances in this field.[1–3]

It has been widely assumed that in low-mobility materials (e.g., amorphous semiconductors, molecular crystals, and conducting polymers) there is high probability that the geminate electron-hole pair will remain bound (an exciton) during the entire thermalization process. Therefore, models of carrier photogeneration for this class of material[4–12] (e.g., the Onsager model)[13] have generally emphasized the importance of the Coulomb interaction between the bound geminate electron-hole pair (exciton), and the role of external field and phonons in the dissociation process of this pair into ''free'' mobile carriers. These models have assumed that the carrier generation is a secondary process resulting from exciton dissociation, and the quantum efficiency was predicted to depend strongly on temperature, photon energy, and external field.[4–12]

However, transient photoconductivity measurements of amorphous selenium (a-Se) in the subnanosecond time region reveal that different phenomena underlie the carrier generation in this system. The experimental facts of particular importance are the following: (i) the fast transient photocurrent is independent of temperature (T); (ii) the fast transient photocurrent is linearly proportional to the external field (E); and (iii) The fast transient photocurrent is linearly proportional to the light intensity (I).

(i) and (ii) imply that the quantum efficiency of carrier generation, η, is independent of T and E. (iii) implies that the carrier generation is independent of the level of excitation (i.e., carriers are generated by a first order process that cannot be attributed to interactions between excitations). The fast transient photoconductivity results suggest that at the earliest time scale accessible (50 ps), the dynamics of carriers at extended band states underlie the prompt photoconduction mechanism in a-Se.

Similar behavior of the quantum efficiency has been observed in anthracene,[3] a system also interpreted in terms of the Onsager model.[6–9] Moreover, Warta and Karl[14] have demonstrated in recent years that the mobility in various molecular crystals (e.g., naphthalene) approaches high values at low temperatures (up to 400 cm^2/Vs). Indeed, these authors have concluded that the carrier transport in these molecular crystals can be understood in terms of a standard band-model description.

In this paper we focus mainly on the carrier generation mechanism in a-Se. Using the MSS measuring technique with a small sample length (microstrip gap size of 6 μm) has facilitated fast transient photoconductivity at high external fields (up to 5×10^5 V/cm) at moderate bias voltages. These measurements at such high fields provide a crucial test of the applicability of the Onsager carrier generation model, which predicts a crossover from a quantum efficiency independent of external field below 10^4 V/cm to one dependent on the field above 10^4 V/cm.[11,12] The present measurements conducted with higher temporal resolution also enable us to resolve the initial decay rate of the transient photocurrent, and to conduct these measurements at very low density of excitation.

Our finding that the quantum efficiency in a-Se is independent of temperature and bias field appears inconsistent with the interpretation of time-of-flight (TOF) and xerographic discharge (XD) experiments that had established the Onsager geminate recombination model.[11,12] In an attempt to unravel the reasons for the different photoconductive responses manifested by these measuring techniques we conducted a comparative study of the photocurrent response in the MSS and the TOF experiments using identical samples (obtained from the Xerox Corporation.). This is particularly

important since all previous studies of the temperature dependence of the quantum efficiency have utilized the TOF technique.[11,12] We will demonstrate that in the TOF measurements, in which the sample is illuminated through a semitransparent metallic electrode, the prompt photoconductance response is greatly influenced by a built-in potential barrier at the semiconductor-metal interface. In fact all the hallmarks of such a potential are revealed experimentally (e.g., photocurrent response at zero bias field, superlinear dependence of the photocurrent on bias voltage, thermally activated photocurrent, etc.).

Moreover, analysis of this comparative study reveals the role of an external field in the various measuring methods. It indicates that in the TOF and XD measurements, the external field, in addition to increasing the drift velocity, effectively separates the positive and negative photocarriers in the absorption region and thereby determines the extent of carrier recombination (i.e., the carrier supply yield), rather than the intrinsic quantum efficiency (defined by the number of carriers produced by an absorbed photon prior to recombination or trapping). The above comparative study also accounts for the experimental observation of a monotonic increase in carrier supply yield with an increased external field in TOF and XD measurements at the entire field regime, including the low-field regime for which it could not be accounted for theoretically by the Onsager model.[11,12,15] We also find the photocurrent response dependent on photon energy, which determines the optical absorption depth and thereby the extent of recombination quenching. In particular, our present TOF experiments verify that at low photon energy, where the absorption depth is large, no significant recombination quenching can be achieved, and as observed in the MSS configuration the carrier supply yield becomes field independent.

In Sec. II we briefly outline the previous models of carrier generation employed for the class of low mobility materials. In Sec. III we describe the MSS and TOF experimental techniques, and in Sec. IV we present our experimental observations. Section V discusses the implications of the experimental data on the mechanisms of carrier generation, carrier recombination, and carrier mobility in *a*-Se, and the various processes underlying the photoconductive response in the MSS, TOF, and XD experiments. Section VI presents a summary of our main findings and concluding remarks.

II. OUTLINE OF PREVIOUS MODELS OF QUANTUM EFFICIENCY FOR THE CLASS OF LOW-MOBILITY MATERIALS

The salient assumption underlying previous models of quantum efficiency for the class of low-mobility materials has been that the geminate carriers remain bound during the entire thermalization process. Consequently, according to these models, at moderate temperatures and external fields, the typical spatial separation, r_0, attained between these carriers at the end of thermalization is smaller than the spatial dimension of the confining potential barrier U (due to the mutual Coulomb interaction and external field). Thus, a carrier needs to surmount this barrier in order to dissociate from its geminate partner and delocalize. The probability of geminate carrier's dissociation (which determines the quantum efficiency) according to these models greatly depends on temperature and external field.

The dissociation process of the geminate carriers was initially described within the framework of the Poole-Frenkel theory,[16] but later, after a few modifications, the Onsager solution was adopted.

Based on Boltzmann statistics, the probability of an electron surmounting a barrier E_0 (at zero applied field) is proportional to $\exp(-E_0/k_BT)$, where k_B is the Boltzmann constant. The Poole-Frenkel[15,16] potential, $U=-e^2/4\pi\epsilon\epsilon_0 r - eEr$ (where e is the electron charge, and $\epsilon\epsilon_0$ is the permittivity of the photoconductor) is reduced by the external field E by the amount ΔE, and the probability of dissociation of the bound electron-hole pair is therefore proportional to $\exp[-(E_0-\Delta E)/k_BT]$. The maximum of the reduction occurs at a spatial separation R where the potential $U=-e^2/4\pi\epsilon\epsilon_0 r - eEr$ is maximum. From $dU/dr=0$ it follows that

$$R=(e^2/4\pi\epsilon\epsilon_0 E)^{1/2},$$

and the total reduction of the potential at R is given by $\Delta E=\epsilon ER=\beta E^{1/2}$, where $\beta=(e3/4\pi\epsilon\epsilon_0)$. Thus, the probability of carrier dissociation is proportional to

$$P_d \approx \exp[-(E_0-\beta E^{1/2})/k_BT]. \tag{1}$$

Tabak and Warter[17] modified this simple model by including a ''nonphotoconductive'' recombination channel of decay. Defining $\tau_e=1/(\nu P_d)$, and τ_r as the lifetimes for escape and recombination, respectively, the resulting steady-state rate equation $dN_p/dt=I_{\rm ph}-N_p/\tau_r-N_p/\tau_e$, where $I_{\rm ph}$ is the photon flux, N_p is the density of excited electron-hole pairs, τ_r^{-1} is the rate of decay of excitation through geminate recombination, and τ_e^{-1} is the rate at which the pairs dissociate into free carriers, suggests that the quantum efficiency is proportional to $\eta=(N_p/\tau_e)/I_{\rm ph}=(1+\tau_e/\tau_r)^{-1}$, where the escape lifetime is

$$\tau_e=\nu^{-1}\exp[(E_0-\beta E^{1/2})/k_BT], \tag{2}$$

and ν is the attempt-to-escape frequency.[10,17]

While the above model could predict the strong dependence of the quantum efficiency on T and E observed in the TOF and XD measurements it could not account for the dependence of the activation energy on photon energy.[12,15] In order to remedy that Knights and Davis[10] introduced some modifications based on the thermalization of hot carriers: a thermalization distance r_0 between the photoexcited electron with excess energy of $\hbar\omega-E_g$ and its hole partner that is attained at the end of thermalization after the electron lost an excess kinetic energy of $\hbar\omega-E_g-E_c$ (where E_g is the bandgap energy and E_c the Coulomb energy of the geminate pair). Assuming a diffusive carrier motion (with a diffusion constant D), and energy-loss rate reaching a maximum value equals the phonon frequency $\nu_{\rm ph}$ times phonon energy $\hbar\nu_{\rm ph}$, the attempt-to-escape frequency ν was taken as the reciprocal of the time taken for the carrier to separate a distance equal to the Coulomb capture radius r_C (where r_C is defined as the separation at which the Coulomb energy equals $2k_BT$),[10,12]

$$\nu^{-1}=r_C^2/D=e^2/(4\pi\epsilon\epsilon_0)^2 4(k_BT)^2 D.$$

Based on these assumptions the derived quantum efficiency is given by

$$\eta=(1+\{e^4/[4\tau_r(4\pi\epsilon\epsilon_0)^2 4(k_BT)^2D]\}\exp(E_a/k_BT))^{-1}, \tag{3}$$

where

$$E_a=e^2/(4\pi\epsilon\epsilon_0 r_0)-4\beta E^{1/2}+eEr_0,$$

and r_0 is defined by

$$2\pi\hbar\nu_{\rm ph}^2 r_0^2/D=(\hbar\omega-E_g)+e^2/(4\pi\epsilon\epsilon_0+r_0)+eEr_0.$$

While the predictions of this model are in qualitative agreement with previous observations, a quantitative agreement is generally not observed over any substantial range of experimental parameters.[12] The most serious discrepancy between the theory and observations lies in the magnitude of β, which is one of the basic parameters in the Poole-Frenkel theory.

The previous method to remedy that was to assume that τ_r is not constant but should be dependent on temperature, through the diffusion velocity, and on r_0. Predicting r_0 however, requires proper modeling of the thermalization process of hot carriers, which at the time was not understood well enough to be uniquely determined. Therefore the reverse approach was chosen, namely, to use r_0 as a parameter in the separation-recombination process, so that if it could be determined as a function of photon energy and temperature from a fit of the experimental observations to the theoretical solution, it would help to develop a model of hot carrier thermalization. This is the approach taken by the Onsager theory.[12]

The original theory Onsager developed was intended for the dissociation process of two oppositely charged ions in a weak electrolyte.[13] But later his solution was adopted for the carrier photogeneration problem in a-Se (Refs. 11 and 12) and in molecular crystal anthracene.[6,18] This classical theory considered only thermalized carriers, and made no assumptions regarding the carrier dynamics during thermalization. The model tacitly assumes that the photocarriers are strongly bound during the entire thermalization process, and reduces to a problem of Brownian motion in the presence of Coulomb attraction and external field. The quantum efficiency according to this model depends on two parameters: the yield of thermalized carriers per absorbed photon, ϕ_0, and the initial separation between thermalized geminate carriers, r_0. The solution provided the probability that at a given external electric field and temperature, a pair of thermalized geminate carriers separated by r_0 would escape geminate recombination (it is assumed that carriers undergoing geminate recombination do not contribute to the photoconductivity). In practice, the parameters ϕ_0 and r_0 were deduced from fitting to the theoretical solution to the experimental results.[6–12,14,15,18]

The Onsager theory involves a solution of the steady-state Smoluchowski diffusion equation in the field[13]

$$U=-e^2/4\pi\epsilon\epsilon_0 r-eEr\cos\Theta$$

for a source at r and sinks at both the origin and infinity. The ratio of the stationary flow into infinity to the flow into the source defines the probability $f(r,\Theta,E)$ that a pair of thermalized carriers initially separated by r and an angle Θ with respect to the electric field direction will escape geminate recombination; this solution is given by[6–12,14,15,18]

$$f(r,\Theta,E)=\exp(-A)\exp(-B)\times\sum_{n=0}^{\infty}\sum_{m=0}^{\infty}(A^m/m!)B^{m+n}/(m+n)! \tag{4}$$

where $A=e^2/4\pi\epsilon\epsilon_0 r k_BT$, and $B=(eEr/k_BT)(1+\cos\Theta)$. Defining $g(r,\Theta)$ as the initial spatial distribution of the thermalized geminate carriers, the derived quantum efficiency is

$$\eta=\phi_0\int f(r,\Theta,E)g(r,\Theta)d^3r.$$

Assuming $g(r,\Theta)$ is an isotropic δ function, $g(r,\Theta)=(1/4\pi r_0^2)\delta(r-r_0)$, Eq. (4) can be integrated; the first few terms of the solution are[18]

$$\eta(E,T,r)=\phi_0\exp[-r_C(T)/r]\{1+(e/k_BT)]r_CE/2!+(e/k_BT)^2(r_C/3!)r_C(r_C/2-r)E^2+(e/k_BT)^3(r_C/4!)(r^2-rr_C+r_C^2/6)E^3+\cdots\}, \tag{5}$$

where the critical Onsager radius, r_C, is defined as the distance at which the mutual Coulomb energy equals k_BT, i.e., $r_C=e^2/4\pi\epsilon\epsilon_0 k_BT$.

The common feature to all the above solutions [Eqs. (1)–(5)] is the prediction of strong dependence of the quantum efficiency on temperature and external field, a prediction that will be directly compared with our experimental observations.

III. METHODS OF MEASURING THE TRANSIENT PHOTOCONDUCTIVITY

A. The MSS measuring technique

The transient photoconductivity is measured using the Auston microwave stripline switch technique.[1] A film of a-Se is deposited on an alumina substrate. The gold microstrips are deposited on top of the a-Se film, leaving a gap of 5 μm between 600-μm-wide microstrips, and a gold ground plane is deposited on to the back surface of the alumina substrate to form a transmission line with 50-Ω impedance. One microstrip is biased with a dc voltage, while the other is connected to the EG&G PAR 4400 boxcar system fitted with a Tektronix S-4 sampling head (with a temporal resolution of 25 ps); the photocurrent is determined from the measured voltage at the 50-Ω input resistance (to ground). A PRA LN105A dye laser system pumped with a PRA LN1000 N_2 laser is used to produce 25-ps pulses at the photon energy range 1.8–2.92 eV. The laser light is unpolarized, and its spectral width is 40 nm. During measurements, the light is focused onto the gap between the microstrips. The overall system temporal resolution is about 50 ps. The low repetition rate of the laser pulses (typically, 0.1–6 Hz) facilitates recovery of the sample into its ground state in the intervals between successive pulses.[19]

The electric field distribution in the gap between the microstrips can be predicted from a solution of the Poisson equation. This solution indicates a uniform electric field near

the surface of the sample at the gap in a direction along the microstrips (similar to the electric field distribution in the gap region of a slot line[20]) and a gradual deviation below the the sample surface. For the thin samples used in the present studies, this deviation is negligible.

Prior to carrier recombination and trapping, the quantum efficiency η is related to the peak photocurrent I_p by the following relationship:

$$I_p=(1-R)(1-e^{\alpha d})e\,\eta N\mu E/L, \tag{6}$$

where R is reflectivity, α the absorption coefficient, μ the mobility, L the length of the sample, d the sample thickness, and N the total number of photons incident on the sample. In practice, because of the finite temporal resolution of the measuring system (Δt) and the carrier recombination and trapping that, following pulsed excitation, reduce the number of free carriers, the measured peak photocurrent represents a time average of the product $n(t)\mu(t)$ during Δt, where $n(t)$ is the total number of carriers that survive recombination; therefore, the inferred η from $I_p$represents a lower bound of the quantum efficiency.

The narrow gap between the microstrips (which defines the sample length) of $L=6$ μm facilitates a high external field at moderate bias voltage and thereby a high photocurrent response at 50 ps (since for a given bias $I_p\sim L^{-2}$).[1] In experiments involving very high electric fields one must carefully consider the possibility of transient Joule heating due to the relatively large transient photocurrent that is generated. Our experiments were carried out under constant peak photocurrent conditions (at levels between 10^{-4} and 10^{-3} A); i.e., as the electric field was increased, the light intensity was decreased so as to keep the peak photocurrent constant. By working at a constant photocurrent, the maximum energy per pulse due to Joule heating was limited to $Q<4\times10^{-10}$ J (note that the linear dependence of I_p on light intensity in a-Se justifies this measuring procedure).

In the following we briefly comment on few factors that may affect the experimental results; more details can be found elsewhere.[1,3,19]

(a) We find uniform illumination of the sample important for eliminating the ''glitches'' in the photocurrent response.[1] In practice this condition may be approached by widening the (Gaussian) laser beam waist so that it substantially overlaps the electrodes; for this illumination profile, it was shown by Auston that the relative photocurrent response to high excitation is similar to low excitation at uniform field.[1]

(b) Measurements using the Auston switch configuration (where the sample is uniformly illuminated) do not exhibit significant effects stemming from an accumulation of space charge in a-Se in the vicinity of the metallic electrodes. This was verified by following a measuring procedure specifically designed for monitoring such effects,[3] at which the peak photocurrent is monitored while the external field is switched on and switched off. These experiments revealed that I_p remains in fact constant while the field is on (rather than monotonically decreasing when space charge is present) and abruptly diminishes when the field is switched off (rather than exhibiting a negative photocurrent due to the remnant field due to the space charge).[3] However, as will be demonstrated in the next section, in the TOF measurements where *all* the photocarriers are created in the vicinity of the metal-photoconductor interface (near the front semitransparent metallic contact), we found the photocurrent strongly influenced by a built-in potential barrier.

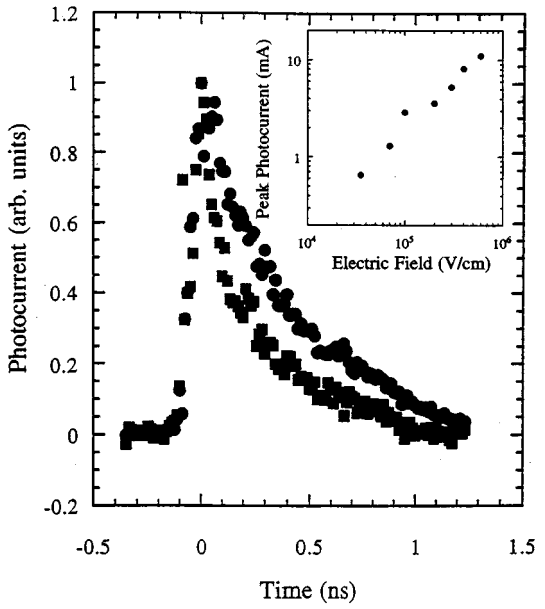

FIG. 1. Wave forms of the normalized transient photocurrent measured in a-Se using the MSS configuration at 20 K (■) and 296 K (●) ($\hbar\omega=2.92$ eV, $E=6\times10^4$ V/cm, and 10^{-7} J/pulse); at $T=296$ K, $I_p=1.45\times10^{-3}$ A; the inset depicts the peak photocurrent dependence on bias field at 296 K.

B. The time-of-flight measuring technique

In order to achieve high temporal resolution, the sample in the TOF measurements is incorporated onto the microstrips.[3] This configuration is constructed by a few successive vacuum depositions onto the top side of the alumina substrate: first the bottom gold electrode, then the a-Se sample, and finally on the top of the a-Se film a semitransparent gold electrode through which the sample is illuminated. The thickness of the sample is 3 μm, and the thickness of the top semitransparent gold electrode is 15 nm. The small overlap area between the top and bottom electrodes ($\cong10^{-3}$ cm^2) minimizes the capacitance of the device, and thereby facilitates a temporal resolution of $\cong1$ ns. As in the MSS configuration, a gold ground plane is deposited on to the back surface of the alumina substrate to form a transmission line with 50-Ω impedance. The top electrode is connected to the boxcar input and the bottom electrode to the bias source.

IV. EXPERIMENTAL RESULTS OF THE TRANSIENT PHOTOCONDUCTIVITY OF a-Se

A. Results in the MSS configuration

Most of the data reported here are from a-Se samples obtained from the Xerox Corporation. The samples prepared by vacuum deposition in our lab exhibit similar transient photoconductivity results.

Figure 1 shows a typical transient photocurrent wave form of the a-Se sample, at two temperatures: 20 and 296 K, normalized at $t=0$. The photocurrent waveform is characterized by a fast initial rise, followed by a fast fall into a small

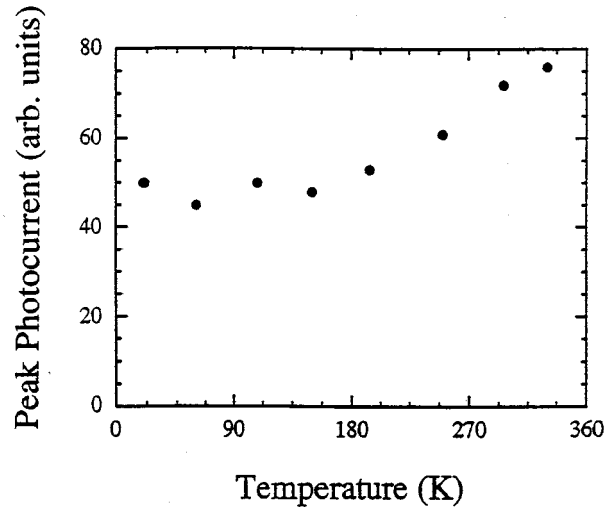

FIG. 2. The temperature dependence of the peak transient photocurrent measured in a-Se using the MSS (at $\hbar\omega=2.92$, $E=6\times10^4$ V/cm).

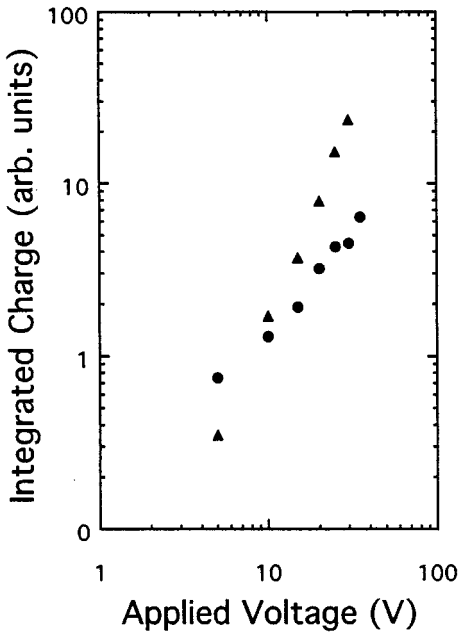

FIG. 3. The dependence of the transient charge Q on positive bias voltage measured in the TOF configuration at two photon energies: 1.8 eV (●) and 2.92 eV (▲).

longer-lived photocurrent tail that disappears at low temperatures. The photocurrent rise time indicates the overall temporal resolution of the measuring system. The photocurrent rate of decay depends on temperature: fitting the data to an exponential form indicates a characteristic decay time of 460 and 170 ps at room temperature and 20 K, respectively.

As shown in Fig. 2, in contrast to the photocurrent tail the magnitude of I_p decreases only slightly at low temperatures. The different temperature dependence of I_p and of the photocurrent ''tail'' indicates that two distinct transport mechanisms dominate the short-and long-lived photocurrent components.

The small gap configuration in the Auston switch (6 μm) is useful for determining the dependence of the photocurrent on the external field in a broad field regime. Our data (depicted in the inset of Fig. 1) indicate a linear dependence of I_p on E up to the highest applied field (5×10^5 V/cm). I_p is found to be linearly dependent on light intensity as well. The magnitude of the peak photocurrent at room temperature, measured at $\hbar\omega=2.92$ eV, $E=6\times10^4$ V/cm, and with energy per pulse of 10^{-8} J is 1.45×10^{-3} A. Using Eq. (6), we find the quantum efficiency to be $\eta=4\times10^{-2}$. Note that this value of η is a lower bound for the quantum efficiency, since, as mentioned above, the measured peak photocurrent is proportional to a time average of the product $n(t)\mu(t)$ during Δt, at a time when n is rapidly decreasing.

Measurements employing the MSS configuration with a larger gap between the microstrips and a laser light focused into a spot smaller than the gap size indicate that the photocurrent response is not very sensitive to the location of the light spot. Also, measurements in which the regions of the metal-semiconductor interface are masked [using the scheme depicted in Fig. 1(c) in Ref. 3] indicate photocurrent response at all temperatures.

In order to measure the photocurrent response at low densities of excitation, we measured the I_p dependence on temperature in a thin a-Se sample (240 nm) at $\hbar\omega=1.8$ eV at moderate field ($E=3\times10^4$ V/cm) with two additional preamplifiers so that the light intensity could be reduced considerably. These measurements at a laser pulse energy smaller than 3×10^{-8} J indicate a prompt transport mechanism that is temperature independent. Considering the relatively small optical absorbance of a-Se at $\hbar\omega=1.8$ eV, we estimate the density of excitation in this experiment to be below 10^{16} cm^{-3}. At higher photon energies, small density of carriers could be obtained in measurements at the high-field regime. These measurements also confirmed the temperature independence of I_p.

B. Results of the TOF measurement

The room-temperature photocurrent wave form (Fig. 5 in Ref. 3) is characterized by a short-lived response associated with the transport of both electrons and holes at the absorption region, followed by a plateau that is associated with transport of one type of carrier that eventually solely remains in the sample, after the other type of carrier has reached the front metallic electrode where it recombined. The plateau indicates that after a short time (on the order of 1 ns) carrier recombination is effectively quenched. The constant photocurrent persists until the photocarrier packet (electrons or holes, depending on the polarity of the external field) reaches the back electrode. The mobilities of electrons and holes as deduced from the measured transit times in our experiments agree with previous results.[11,12]

As will be discussed in the next section, at a photon energy at which the absorption depth is relatively small, the onset of recombination quenching depends on the external field, whereas for relatively thick samples, uniformly excited, no effective recombination quenching can be achieved. In order to verify this we measured the transient photocurrent in the TOF configuration at two photon energies: 2.92 and 1.8 eV. Figure 3 indeed shows that at 1.8 eV, at which the light absorption is almost uniform across the relatively thick

sample (3μm), the integrated charge Q (obtained from integrating the transient photocurrent wave form) is almost linearly dependent on E ($Q\sim E^{1.05}$), whereas at 2.92 eV, at which the absorption depth is much shorter, it depends superlinearly on E ($Q\sim E^{1.97}$).

The observation of a photocurrent response at zero applied field (when both electrodes are grounded) in our TOF experiments (Fig. 6 in Ref. 3) reveals unambiguously the existence of a built-in potential at the metal-semiconductor interface. At relatively low light intensity, only a negative transient photocurrent is detected, but at higher light intensity a longer-lived positive transient photocurrent appears. The photocurrent wave form seems to be the sum of these two responses.

The transient photocurrent depends on the polarity of the external voltage in the following way: as a positive voltage is applied, the positive component of the photocurrent detected at zero bias increases, while the negative photocurrent component decreases and eventually diminishes (at $+2$ V). The opposite behavior is observed at a negative external voltage polarity. The negative photocurrent component increases with an increased field while the positive component diminishes (at -2 V). At $V>2$ V, when excited with photon energy of 2.92 eV, I_p as well as Q increases superlinearly with V.

The peak photocurrent in the TOF configuration exhibits a thermally activated behavior,[3] where the activation energy for the positive photocurrent is about 0.16 eV. In this configuration, the peak photocurrent varies sublinearly with light intensity, as $I_p\cong I^{0.5}$.

Finally, we note that the dependence of I_p on photon energy in the TOF configuration is significantly stronger than the one in the MSS configuration. This greater sensitivity to photon energy in the former case is in agreement with previous TOF measurements,[11,12] which revealed a ratio of the photocurrent at 2.92 and 1.9 eV of about 10^4, significantly larger than the one (8.5) observed in the MSS configuration.[3]

V. DISCUSSION

A. Photoconductivity results in the MSS configuration

As Fig. 1 indicates, the transient photoconductivity in a-Se consists of two distinct transport mechanisms: a relatively short-lived temperature independent one and a long-lived thermally activated one, we associate with a carrier dynamics while occupying extended band states as well as states near the band edges while the carriers tunnel progressively into lower states, and a phonon-assisted multiple trapping transport at band tails, respectively.

Before discussing any other implications of the data, we address the question of the possibility of the sample heating due to the laser light in our experiments. Considering the various experimental observations obtained using the MSS measuring configuration, we have concluded that the temperature-independent initial transient transport is an intrinsic property of a-Se, and that the sample heating due to the laser light is rather small, estimated to be on the order of 1 K. The following observations support this conclusion:

(1) In many materials (e.g., a-Se, conducting polymers, C_{60}, etc.) the transient photocurrent wave form evolves continuously as the sample temperature is reduced. In particular, as the temperature approaches zero the photocurrent tail diminishes.

(2) Measurements of I_p at a reduced light intensity ($\hbar\omega=1.8$ eV) with increased sensitivity (that is facilitated by two additional preamplifiers) verify a temperature-independent prompt transport mechanism at a density of excitation between 10^{14} and 10^{16} cm^{-3}, which we estimate to be too small to cause any significant sample heating.

(3) The transient photoconductivity in ''conventional'' semiconductor single crystals such as GaAs, InP, and anthracene[2] manifests the expected increased of I_p at low temperatures due to the variation of the mobility. Also, transient photoconductivity measurements on materials undergoing structural phase transition, such as polydiacetylene-TS (Ref. 21) and oxygen-free C_{60},[22] reveal a signature of this phase transition (typically in the form of a maximum of I_p) at the correct transition temperatures (known from other independent measurements such as x-ray diffraction, etc.).

The observation of temperature-independent photoconductivity at the earliest time accessible (50 ps) suggests that both the quantum efficiency and prompt mobility in a-Se are temperature independent. A temperature-independent prompt mobility resembles the carrier dynamics in amorphous metals. This carrier dynamics is different from the one exhibited by the thermally activated mobility usually observed in TOF experiments, which reflects the carrier dynamics at relatively long times after excitation (typically at $t>0.1\mu$s) when multiple trapping transport prevails.

The linear dependence of I_p (as revealed by the MSS measurements) and drift velocity (as revealed by the TOF measurements) on external field indicates that the quantum efficiency in a-Se must be field independent (up to the maximum applied external field in our experiment, of 5×10^5 V/cm). This observation, however, does not accord with the Onsager model, and in particular with the predicted monotonic increase of the quantum efficiency with the field above 10^4 V/cm.[11,12] A detailed discussion of the superlinear dependence of the carrier supply yield on the field in the TOF and XD measurements presented in the next section indicates that it originates from the increased supply yield rather than increased quantum efficiency. It is noteworthy that previous TOF and XD measurements also disagree with the Onsager model at low field regime ($E<10^4$ V/cm) where they reveal a carrier supply yield increasing monotonically with E, contradistinctive with the theoretical prediction of field-independent quantum efficiency.[11,12]

Generally, during Δt, the contribution of the phonon-assisted multiple-trapping transport[23] to the transient photocurrent is evidently small as indicated by the weak dependence of I_p on temperature (see Fig. 2). At the low-temperature regime this contribution is negligible as carriers ''freeze'' at traps. The decay of the transient photocurrent at this temperature regime follows an exponential form, indicative of monomolecular recombination kinetics. The relatively small contribution of the multiple trapping transport mechanism to the prompt photoconductivity response at higher

temperature is indicated by the slower rate of decay of the transient photocurrent and the appearance of a small long-lived photocurrent tail. At these temperatures, at a relatively long time after excitation ($t>300$ ps) the transport via multiple trapping (i.e., carrier capture at localized states and phonon assisted carrier release into extended band states) eventually prevails. The characteristic activation energy, $E_{\rm ac}$, associated with this transport mechanism is time dependent; $E_{\rm ac}$ increases with time while the carriers relax progressively into deeper traps. Similar behavior has been observed in other low-mobility systems such as conducting polymers[19,21] and C_{60}.[22]

The observed linear dependence of a transient photocurrent on light intensity implies that the quantum efficiency is independent of the level of excitation (i.e., carriers are generated by a first order process (e.g., interband transition) and cannot be attributed to interactions between excitations).

The action spectrum of I_p in conjunction with the optical absorption spectrum in a-Se (Refs. 10–12) reflects its electronic band structure. As expected, higher photoconductivity is exhibited at higher photon energies as more carriers are excited above the mobility edge.

The above data suggest the following scenario of carrier generation in a-Se. Upon pulsed photoexcitation these processes may take place: (1) Hot carrier thermalization into a Fermi-Dirac distribution. (2) Carrier relaxation to the band edges. (3) Carrier recombination. (4) Carrier trapping at localized states at band tails. Some of these processes may proceed simultaneously. But promptly after excitation, while carriers occupy states above the mobility edge, the contribution of the long-lived transport mechanism associated with phonon-assisted multiple trapping is evidently small, as inferred from the relatively small variation of I_p with temperature. It is noteworthy that other independent measurements have also revealed the existence of hot carriers in various low-mobility materials.[24,25] Generally, the distinct features of transient photoconductivity in a-Se, as compared to crystalline semiconductors, derives from the existence of traps and disorder that significantly reduce the mobility and prolong the transient transport, as evidenced by the appearance of a temperature-dependent long-lived photocurrent tail.

The inapplicability of the Onsager geminate recombination model is perhaps not surprising since this model might be appropriate for strictly localized excitations, rather than for excitations at energy levels above the mobility edge. We note that in conducting polymers, where the broad π bands of conjugated polymers tend toward extensive delocalization, the Onsager geminate recombination model is inapplicable as well.[19,21] This classical model appears more appropriate for describing phenomena involving localized carriers, such as discharge processes following corona charging via a dark current, a phenomenon to which this model has been applied as well.[15] The dark transport in this case involves carrier emission from deep traps into energy levels above the mobility edge, and is indeed characterized by thermally activated behavior.[15]

B. Results of the TOF experiments

The TOF measurements exhibit a qualitatively different transient transport than the one observed in the MSS configuration. The former experimental results are characterized by the following observations: photocurrent response at zero external field, strong dependence of I_p on V, thermally activated I_p, and I_p's great sensitivity to photon energy. These characteristics, which are the hallmarks of photoconductivity in photodiodes, clearly indicate the existence of a built-in potential barrier at the semiconductor-metal interface that strongly affects the carrier transport,[3] in particular since all the carriers are excited at this interface and must confront this potential barrier.

The superlinear dependence of the carrier supply yield on an external field in the TOF measurements appears to originate from two distinct effects. The first effect is due to the quenching of the carrier recombination. As mentioned in Sec. IV B, the initial transient photocurrent in the TOF arises from the motion of both electrons and holes at the absorption region, at which time it decays mostly via carrier recombination. When excited at a spectral region where the absorption coefficient is relatively large (and the absorption depth is relatively small) one type of carrier (either electrons or holes) is eventually eliminated from the sample (as it has completed traversing the absorption region and recombined at the front metallic electrode). At this time carrier recombination is effectively quenched, as manifested by the characteristic plateau seen in the TOF photocurrent wave form.[3,12] However, the onset of recombination quenching depends on the external field, since at a higher field the carriers aiming toward the front contact are driven faster out of the sample. Consequently, in this case, the onset of recombination quenching occurs faster, resulting in a higher number of carriers of the opposite charge that survive recombination. Thus, the field in the TOF measurements determines the ''carrier supply yield'' rather than the intrinsic quantum efficiency (defined as the total number of carriers created by an absorbed photon, prior to recombination).

In an experiment designed to verify this, the transient photoconductivity in the TOF configuration was measured at two photon energies: 2.92 and 1.8 eV. The results depicted in Fig. 3 indicate that in the former case, where the absorption depth is relatively small, the integrated charge Q depends superlinearly (almost quadratically) on V, since that in addition of the transient photocurrent increasing with V due to the larger drift velocity v_d, the number of carriers escaping recombination in the photoconductor increases also with V as the recombination quenching occurs at progressively shorter times (that are inversely proportional to v_d). In contrast, at a photon energy of 1.8 eV almost linear dependence of I_p on V is observed. This latter behavior, which is similar to the one observed in the MSS configuration, can be understood by noticing that at this photon energy the absorption depth is large ($1/\alpha$ is greater than the sample thickness of 3 μm) and thus recombination quenching cannot be achieved in the range of the bias voltage used in our experiments ($V<10^6$ V/cm), since the lifetime of the carriers is shorter than the time required for the carriers aiming toward the front electrode to traverse the sample.

The second effect contributing to the superlinear dependence of the transient photocurrent on V in the TOF experiment may originate from the existence of a potential barrier at the semiconductor-metal interface, as indeed verified by various models of transport through a potential barrier (e.g., transport in photodiodes, thermionic emission, etc.).[26]

The dependence of I_p on light intensity I (i.e., I_p proportional to $I^{0.5}$) suggests a bimolecular recombination kinetics in the TOF measurements. In this measurement, the longer photocurrent rise time ($\Delta t \cong 1$ ns) results in a greater contribution by the multiple-trapping transport to the initial photocurrent response. Therefore, a weaker dependence of I_p on light intensity occurs in the TOF measurements, consistent with the sublinear dependence of the photocurrent tail on light intensity found in measurements employing the MSS configuration.[19,21]

Finally, the much greater sensitivity of I_p on photon energy in the TOF measurements, as compared with that in the MSS measurements,[3] suggests that it may arise from similar processes underlying the superlinear dependence of Q versus V. Thus, at higher photon energies, for which the absorption depth is comparatively small, recombination quenching at a given applied voltage can be attained faster and thus result in a higher carrier supply yield, as compared with the one generated at low photon energies. In addition, a higher current is expected at higher photon energies, as the carrier excited at higher energy levels is more likely to surmount the built-in potential barrier at the metal-semiconductor interface.

C. Comparing previous and present experimental observations

The carrier supply yield (rather than the quantum efficiency) in a-Se, as inferred from TOF and XD (Refs. 11 and 12) measurements, appears to depend strongly on temperature, electric field, and photon energy, characteristics that are qualitatively different from the temperature-and the field-independent quantum efficiency revealed by the MSS measurements. In the following we explore additional factors that distinguish these measuring techniques, and in particular those pertaining to the XD.

An important experimental factor distinguishing the various measuring methods is the temporal resolution. The typical temporal resolution in TOF and XD measurements is from submicrosecond to millisecond. Therefore, the photoconductivity manifested by these measurements is greatly influenced by the temperature-dependent, long-lived transport mechanism.

In Sec. V B we discussed the distinct role played by the external field on recombination quenching as well as the effect of the built-in potential on the photocurrent response in the TOF measurements. Similar effects due to the external field are expected to occur also in the XD experiment. In this ''contactless'' experiment the bias field is created by charging the sample (e.g., corona charging). In order to retain the charge for a sufficiently long time, the photoconductor must have a large density of deep surface traps. After charging, the sample in the XD experiment is discharged by a steady-state monochromatic illumination, as the photocarriers recombine with the localized charges. The rate of discharge is therefore a measure of the photocarrier's supply into the surface region; this photocarrier supply is inferred experimentally from the decay of the surface potential.[11,12,15] In the XD experiment, the attainment of recombination quenching is also expected to depend on the surface potential and the photon energy for similar reasons to those discussed in regard to the TOF measurement. So, once again, we expect the XD experiment to reveal the carrier supply yield rather than the quantum efficiency, in contrast to the MSS experiment in which the uniform excitation of a relatively long sample prevents the attainment of field-induced recombination quenching.

It has been acknowledged previously[11,12,15] that a monotonic increase in the photocarrier supply yield upon increasing the field observed in both the TOF and XD measurements disagrees with the prediction of the Onsager model of a constant quantum efficiency below 10^4 V/cm. This discrepancy was attributed previously to surface recombination.[11,12] Such a suggestion appeared to be supported by a TOF experiment in which the carrier generation was accomplished by second-harmonic excitation. Since the quantum efficiency in this experiment was found to be independent of bias field it was considered an indication of a ''bulk behavior''.[11,12] However, it is noteworthy to point out that in this experiment the small optical absorbance at the fundamental wavelength results in almost uniform excitation profile across the sample, a situation that prevents the attainment of recombination quenching. Thus, this excitation profile is expected to result in a field-independent carrier supply yield.

Considering the various processes underlying the TOF, XD, and MSS experiments, we can reconcile the different experimental observations and conclude that they are not inherently in conflict. But it is important to realize the respective utilities of each experimental technique. While the measurement employing the MSS sample configuration appears adequate for studying the prompt carrier dynamics and the intrinsic properties of the carrier quantum efficiency, the TOF method seems better suited for measuring the mobility (usually at $t > 10^{-9}$ s). The experimental configuration used in both the TOF and the XD experiments, where the electrons and hole can be effectively separated by the external field, are useful for obtaining high photocarrier supply yield in a measuring configuration similar to the one used in electrophotography.[4,15]

VI. SUMMARY AND CONCLUDING REMARKS

Studies of fast transient photoconductivity in a-Se reveal two distinct transport mechanisms. The first is a short-lived one due to carrier dynamics at extended band states and at states near the band edges where the carrier tunnels progressively into lower states. The second is a long-lived one due to multiple trapping at band tails. We find the quantum efficiency in this prototypic low-mobility system independent of temperature and electric field up to the largest applied field of 5×10^6 V/cm, inconsistent with the Onsager model which predicts a strong dependence of the quantum efficiency on both field and temperature. While this and other previous models emphasize the role of external fields and phonons in the dissociation process of thermalized geminate photocarriers, our observations at the earliest time accessible (50 ps) indicate that carrier photogeneration in a-Se occurs while the excitations are delocalized.

Fast transient photoconductivity measurements provide a window for measuring the carrier dynamics at extended band states in amorphous semiconductors. We find the prompt carrier mobility in a-Se independent of temperature, qualitatively different than the thermally activated mobility associated with multiple-trapping transport prevailing at longer time scales that usually prevails in TOF experiments.

The high-field capability enables measurements at low density of excitation. We find the linear dependence of the photocurrent on light intensity persisting at a density of excitation below 10^{16} cm^{-3}, which is smaller than the density at which exciton condensation into electron-hole droplets usually occurs in crystalline semiconductors.

Analysis of a comparative study of transient photoconductivity in the TOF and MSS sample configurations unravels the distinctly different processes underlying the photocurrent responses in various measuring methods (MSS, TOF, and XD). The analysis indicates that it is the carrier supply yield rather than the intrinsic quantum efficiency that can be inferred from TOF and XD experiments. We have demonstrated that the carrier supply yield observed in the TOF and XD measurements depend strongly on the external field since the external field modifies the onset of carrier recombination quenching. In contrast, in the MSS configuration, where a relatively long sample is excited uniformly, the effect of the external field on the carrier recombination appears to be negligible, consistent with similar observations made previously in TOF measurements when the sample was excited uniformly via second harmonic generation. We find the carrier recombination quenching by the external field in the TOF and XD measuring configurations useful for obtaining high carrier supply yield, whereas the MSS measuring configuration is better suited for investigating the prompt carrier dynamics and the intrinsic properties of the quantum efficiency.

Another factor that influences the photocurrent in the TOF experiments has been traced to the existence of a built-in potential barrier at the photoconductor-metal interface. In fact, all the hallmarks of such a potential barrier are manifested in this measuring configuration: photocurrent response at zero bias field, thermally activated photoconductivity, greater sensitivity to photon energy, and strong dependence of the photocurrent on the bias field. However, it appears that this built-in potential barrier does not affect significantly the photocurrent response in experiments employing the MSS sample configuration.

Finally we note that some important questions remain open; in particular the magnitude of the mobility in the subpicosecond time regime, as well as the properties of the quantum efficiency in systems characterized by very small mobility, i.e., $\mu \ll 1$ cm^2/V s. Measurements of transient photoconductivity and mobility in the subpicosecond time regime will be crucial for addressing these fundamental questions.

ACKNOWLEDGMENTS

We are most grateful to D. M. Pai for providing some of the amorphous selenium samples used in our studies and to Omri Moses for proofreading the manuscript. This research was supported partially by the National Science Foundation under NSF-DMR93-00366.

[1] D. H. Auston, J. Quantum Electron. **3**, 636 (1983).
[2] D. Moses, Solid State Commun. **69**, 721 (1989).
[3] D. Moses, Philos. Mag. B **66**, 1 (1992).
[4] D. M. Pai and B. E. Springett, Rev. Mod. Phys. **65**, 163 (1994).
[5] N. F. Mott and E. A. Davis, *Electronic Processes in Non-Crystalline Materials* (Clarendon Press, Oxford, 1979).
[6] M. Pope and C. E. Swenberg, *Electronic Processes in Organic Crystals* (Clarendon Press, Oxford, 1982).
[7] E. A. Silinsh, *Organic Molecular Crystals. Their Electronic States* (Springer-Verlag, Heidelberg, 1980).
[8] K. c. Kao and W. Hwang, *Electronic Transport in Solids* (Pergamon Press, Oxford, 1981).
[9] R. G. Kepler, in *Tretise On Solid State Chemistry*, edited by N. B. Hannay (Plenum, New York, 1976), Vol. 3.
[10] J. C. Knights and E. A. Davis, Phys. J. Chem. Solids **35**, 543 (1974).
[11] D. M. Pai and R. C. Enck, Phys. Rev. **11**, 5163 (1975).
[12] R. C. Enck and G. Pfister, in *Photoconductivity and Related Phenomena*, edited by J. Mort and D. M. Pai (Elsevier, Amsterdam, 1976).
[13] L. Onsager, Phys. Rev. **54**, 554 (1938). A recent theoretical extension of the Onsager solution has been developed by H. Scher and S. Rackovsky, J. Chem. Phys. **81**, 1994 (1984).
[14] W. Warta and N. Karl, Phys. Rev. B **32**, 1172 (1985).
[15] M. Scharfe, *Electrophotography Principles and Optimization* (Research Study Press, John Wiley, New York, 1984).
[16] J. Frenkel, Phys. Rev. **2**, 599 (1934).
[17] M. D. Tabak and P. J. Warter, Phys. Rev. **173**, 899 (1968); E. A. Davis, J. Non-Cryst. Solids **4**, 107 (1970).
[18] R. R. Chance and C. L. Braun, J. Chem. Phys. **59**, 2269 (1973).
[19] D. Moses and A. J. Heeger, in *Relaxation in Polymers*, edited by T. Kobayashi (World Scientific, Singapore, 1993).
[20] K. C. Gupta, *Microwaves* (Wiley, New Delhi, 1979); F. Gardiol, *Introduction to Microwaves* (Artech House, Dedham, MA, 1984).
[21] D. Moses, M. Sinclair, and A. J. Heeger, Phys. Rev. Lett. **58**, 2710 (1987).
[22] C. H. Lee, G. Yu, B. Kraabel, D. Moses, and V. I. Srdanov, Phys. Rev. B **49**, 10 572 (1994).
[23] M. A. Kastner, in *Physical Properties of Amorphous Materials*, edited by D. Adler, B. B. Schwartz, and M. C. Steele (Plenum, New York, 1985).
[24] Z. V. Vardeny and J. Tauc, in *Semiconductors: Probed by Ultra Fast Laser Spectroscopy*, edited by R. R. Alfano (Academic, New York, 1984), Vol. II.
[25] J. R. Andrew, T. E. Orlowski, H. Gibson, M. L. Slade, W. Knox, and B. Wittsmershaus, Phys. Rev. B **27**, 6545 (1983).